

Image-Specific Information Suppression and Implicit Local Alignment for Text-based Person Search

Shuanglin Yan, Hao Tang, Liyan Zhang and Jinhui Tang

arXiv:2208.14365v1 [cs.CV] 30 Aug 2022

Abstract—Text-based person search is a challenging task that aims to search pedestrian images with the same identity from the image gallery given a query text description. In recent years, text-based person search has made good progress, and state-of-the-art methods achieve superior performance by learning local fine-grained correspondence between images and texts. However, the existing methods explicitly extract image parts and text phrases from images and texts by hand-crafted split or external tools and then conduct complex cross-modal local matching. Moreover, the existing methods seldom consider the problem of information inequality between modalities caused by image-specific information. In this paper, we propose an efficient joint Information and Semantic Alignment Network (ISANet) for text-based person search. Specifically, we first design an image-specific information suppression module, which suppresses image background and environmental factors by relation-guide localization and channel attention filtration respectively. This design can effectively alleviate the problem of information inequality and realize the information alignment between images and texts. Secondly, we propose an implicit local alignment module to adaptively aggregate image and text features to a set of modality-shared semantic topic centers, and implicitly learn the local fine-grained correspondence between images and texts without additional supervision information and complex cross-modal interactions. Moreover, a global alignment is introduced as a supplement to the local perspective. Extensive experiments on multiple databases demonstrate the effectiveness and superiority of the proposed ISANet.

Index Terms—Text-based person search, information inequality, image-specific information, modality-shared semantic topic centers, implicit local alignment.

I. INTRODUCTION

PERSON re-identification (Re-ID) is a hot research topic in computer vision, which aims to retrieve the given query object from the gallery set collected across cameras. Depending on the data type of the query object, person re-identification can be broadly divided into three subtasks, image-based Re-ID [1]–[3], video-based Re-ID [4]–[6], and text-based person search [7]. In the past decade, image-based Re-ID and video-based Re-ID have attracted extensive attention in academia and industry, and impressive progress has been made. Compared with the above two sub-tasks, text-based person search can search the target object with a simpler and more accessible text description. Due to its great practicability, text-based person search has received increasing attention in recent years.

S. Yan, H. Tang and J. Tang are with the School of Computer Science and Engineering, Nanjing University of Science and Technology, Nanjing 210094, China (e-mail: shuanglinyan@njust.edu.cn; tanghao0918@njust.edu.cn; jinhuitang@njust.edu.cn).

L. Zhang is with the College of Computer Science and Technology, Nanjing University of Aeronautics and Astronautics, Nanjing 210016, China (e-mail: zhangliyan@nuaa.edu.cn).

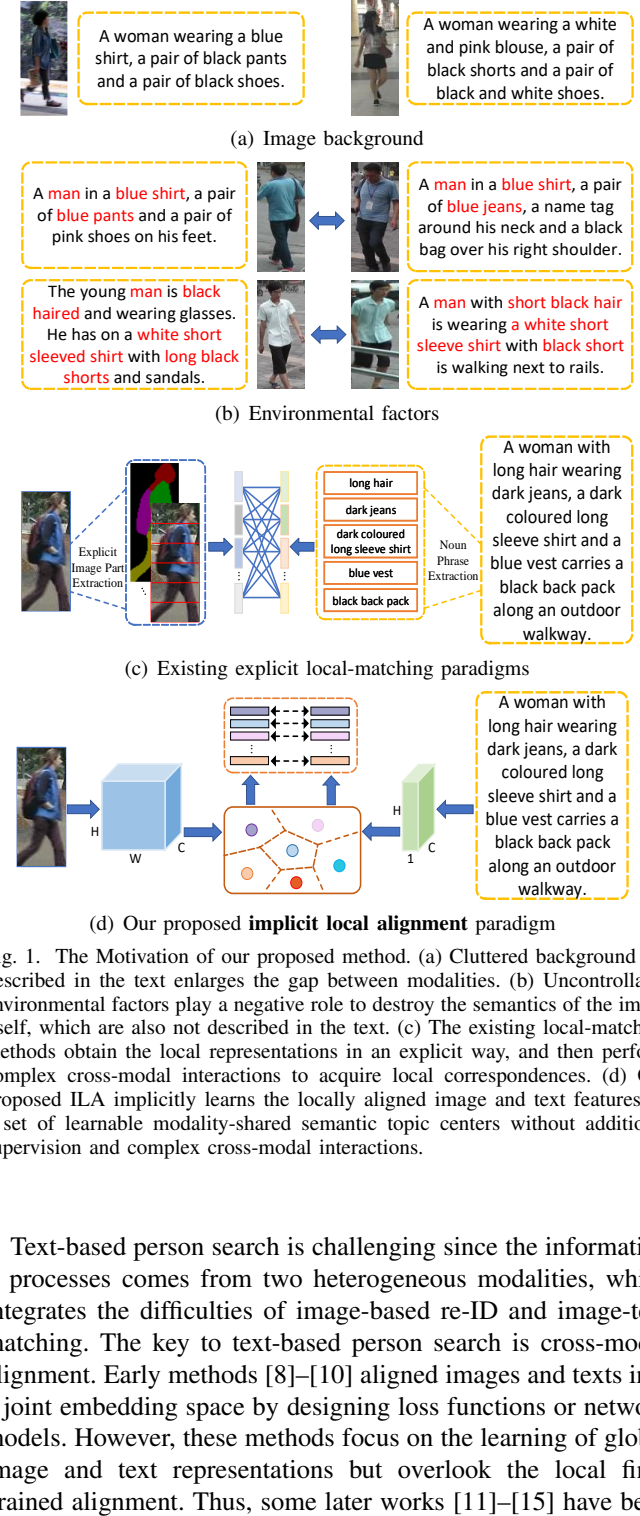


Fig. 1. The Motivation of our proposed method. (a) Cluttered background not described in the text enlarges the gap between modalities. (b) Uncontrollable environmental factors play a negative role to destroy the semantics of the image itself, which are also not described in the text. (c) The existing local-matching methods obtain the local representations in an explicit way, and then perform complex cross-modal interactions to acquire local correspondences. (d) Our proposed ILA implicitly learns the locally aligned image and text features by a set of learnable modality-shared semantic topic centers without additional supervision and complex cross-modal interactions.

Text-based person search is challenging since the information it processes comes from two heterogeneous modalities, which integrates the difficulties of image-based re-ID and image-text matching. The key to text-based person search is cross-modal alignment. Early methods [8]–[10] aligned images and texts into a joint embedding space by designing loss functions or network models. However, these methods focus on the learning of global image and text representations but overlook the local fine-grained alignment. Thus, some later works [11]–[15] have been

proposed to perform local image-text matching. The general process is to first explicitly obtain local representations of image and text, and then establish the local correspondence between them, as shown in Figure 1(c). To obtain local representations of images and texts, the most common strategy is to directly splitting image and text [13]–[15]. There are also some works [11], [12] introduced external tools to acquire local representation, such as human body keypoint detector, human parsing, and the Stanford POS tagger [16]. However, such explicitly acquired local features are unreliable, which can corrupt the contextual information of images and texts or introduce noise. For learning the local fine-grained correspondence between image and text parts, the most popular strategy [13], [14] is to perform complex cross-modal interact operations. The strategy can achieve superior retrieval performance, but it requires a high computational cost due to the expensive pairwise interact operation.

In addition, most existing methods directly encode the original images and texts in the same way to obtain image and text embeddings, without considering the modality-specific information in the image. The text only describes the appearance information of pedestrian, and the image is captured by the surveillance camera, it inevitably contain some information about the surrounding environment that is not described in the text. These environmental information plays a role of noise for image-text alignment, which leads to information inequality between image and text, and increases the difficulty of cross-modal alignment. According to our observation, the problem is mainly caused by the following two kinds of image-specific information: (1) **Image background**, as shown in Figure 1(a). Cross-modal alignment only focuses on the common information between modalities, while image background that is not described in the text undoubtedly enlarges the gap between modalities as noise. (2) **Environmental factors**, such as illumination, weather, etc., as shown in Figure 1(b), which is not only a kind of noise, but even destroy the semantics of the image itself, resulting in great intra-class variations.

The above observations motivate us to design a lightweight model to suppress image-specific information and implicitly learn the locally aligned image and text features. In this paper, we propose a joint Information and Semantic Alignment Network (ISANet) for text-based person search. As shown in Figure 2, it consists of an Image-Specific Information Suppression (ISS) module to alleviate the influence of image-specific information and achieve cross-modal alignment at the information level, an Implicit Local Alignment (ILA) and a Global Alignment (GA) module to implicitly learn the locally and globally aligned features at the semantic level. Specifically, ISS first introduces a Relation-Guide Localization (RGL) submodule to model the global context information of image and fully understand the image semantics to highlight the modality-shared human body region. Then, a Channel Attention Filtration (CAF) submodule is introduced, which employs instance normalization and channel attention to filter environmental factors while avoiding the loss of identity information. The Implicit Local Alignment (ILA) module implicitly learns the locally aligned image and text features, as shown in Figure 1(d). In order to achieve this goal, we first introduce a set of learnable semantic

topic centers, which are shared between two modalities, and then calculate the relationship between each pixel feature of image or each word feature of text and these topic centers. Finally, their corresponded relationship is used as the soft-assign weight to aggregate the image and text features to each semantic center to generate the implicitly aligned local image and text features. The Global Alignment (GA) module aggregates image salient information spatially and text salient information temporally, and then maximizes the similarity between them in a joint embedding space for global alignment. The above modules are integrated and joint optimized in an end-to-end manner. It is worth noting that the proposed ISANet does not require any additional supervision information and complex cross-modal interact operations. With the above work, the features extracted by ISANet are cross-modal aligned at the information and semantic levels, and the similarity between features can be directly measured during inference for text-to-image retrieval. Our main contributions can be summarized as follows:

- Firstly, an image-specific information suppression module is designed to alleviate information inequality between modalities and achieve information alignment between images and texts. It includes relation-guide localization and channel attention filtration to suppress image background and filter environmental factors respectively, and introduces an identity-relevant content consistency loss to avoid the loss of identity information in the filtering process.
- Secondly, an implicit local alignment module is proposed to implicitly learn the locally aligned image and text features. We aggregate image and text into a set of shared semantic topic centers to reduce the semantic gap between images and texts. To our best knowledge, we are the first to implicitly learn local features for modal alignment in an end-to-end way for text-based person search.
- Finally, we have conducted extensive experiments on two databases to verify the effectiveness of the proposed model, i.e., CUHK-PEDES and ICFG-PEDES. The results show significantly improvement on two databases, and the performance significantly outperform the existing methods.

The remainder of the paper is organized as follows: Section II reviews the works related to the present paper; Section III describes the proposed model in detail, followed by objective function; Section IV shows extensive experimental results and analysis; and finally the paper is summarized in Section V.

II. RELATED WORK

A. Text-based Person Search

The task of text-based person search was first proposed by [7], and released the first large-scale person description (CUHK-PEDES) database, which greatly promoted the development of the task. The core problem is the modality alignment between images and texts. To solve the problem, a series of methods have been put forward in recent years. Some early works [7]–[10], [17] mainly focused on the global matching between image and text. Among them, Chen *et al.* [10] also considered the problem of information inequality between images and texts, and proposed a cross-modal knowledge adaptation method to solve the problem by directly adapt the knowledge of images

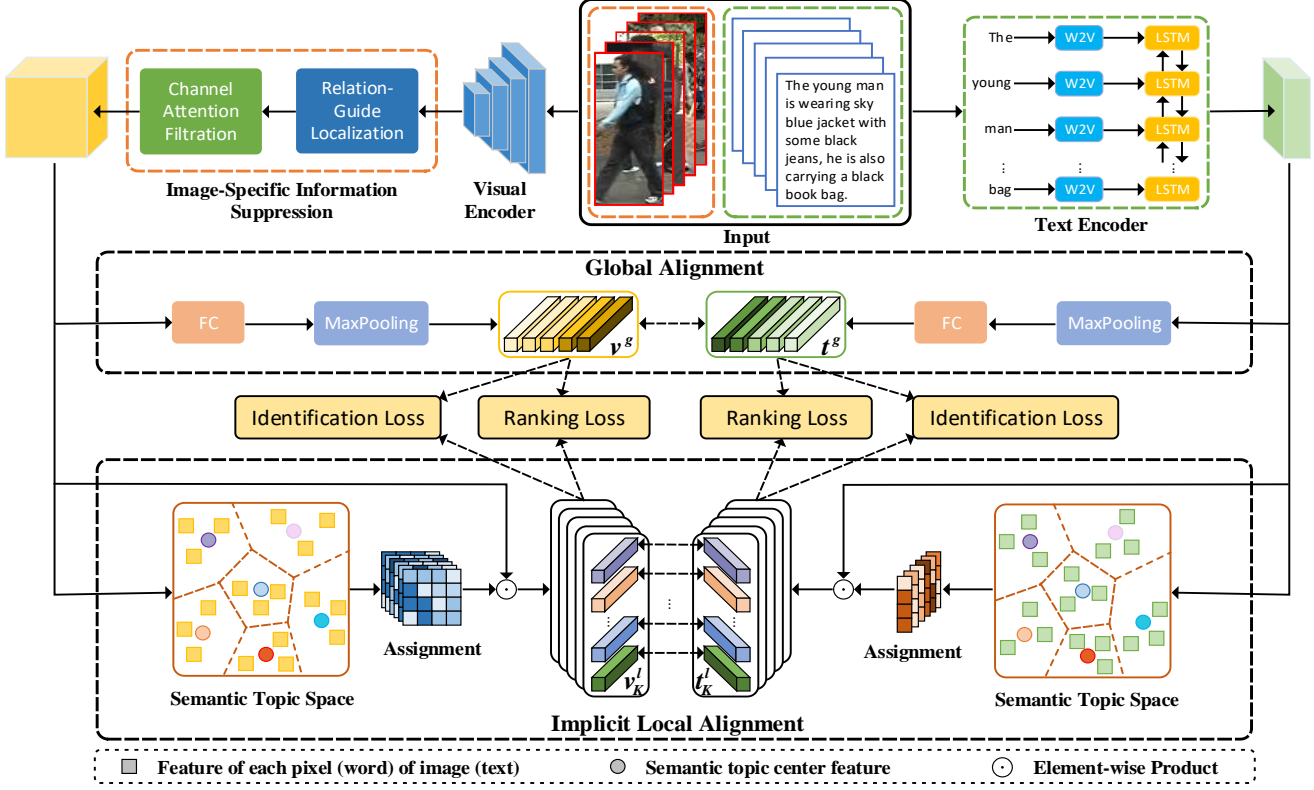


Fig. 2. Overview of the proposed ISANet. Given image-text pairs, we extract image and text feature maps by image and text encoder respectively. We feed the image feature map to an image noise suppression module to eliminate the effects of image background and environmental factors through relation-guide localization and channel attention filtration respectively. The output image features and text features are sent to the global and local semantic alignment branches respectively. In the global branch, the image and text features are respectively encoded into a joint embedding space through two fully connected layers for global alignment. In the local branch, we design a set of shared learnable semantic topic centers, and then respectively calculate the assignment of image and text features to each center, and finally aggregate the image and text features based on the assignments to generate the locally aligned image and text features. The generated global and local features for images and texts are supervised by Ranking loss and Identification loss to achieve information and semantic alignment.

to the knowledge of texts at three different levels. However, it is unreasonable to adapt image to text directly due to the semantic gap between modalities. Different from [10], we use attention mechanism to explicitly suppress image-specific information. Moreover, the above methods only focus on global representations, which may miss some distinctive local details or mix a little noise information.

To mine local distinctive detail information, a lot of works [11]–[15], [18]–[23] has focused on exploring local matching between images and texts. Some efforts work on more effective mechanisms to probe the cross-modal association. Niu *et al.* [19] designed a hierarchically multi-granularity image-text matching mechanism, i.e., global-global, global-local and local-local, to achieve more accurate similarity evaluation. Beyond this, some works [11], [12], [20] introduced external information to assist in exploring local features. Wang *et al.* [11] introduced the semantic attribute as a bridge to mine the local visual attribute features and textual attribute phrases, and build association between them by a k-reciprocal sampling align loss. Recently, some effective and lightweight models [15], [23] have been proposed, and achieved the state-of-the-art performance. SSAN [15] designed a word attention module to attend to part-relevant words with the image part feature as guide, and proposed a compound ranking loss to overcome the large intra-class variance in textual descriptions. These local-matching methods all

acquire local features explicitly, which will destroy the complete context information of images and texts and even introduce noise. Unlike them, we implicitly learn local aligned features by aggregate image and text into a set of shared semantic topic centers, without complex cross-modal interaction.

B. Image-Text Embedding

For cross-modal retrieval tasks, it is vital to learn an effective embedding space. In the embedding space, two modalities can be fully understood, and the semantic gap between modalities can be effectively alleviated. Some early works [8], [9], [24] focus on designing network and optimization loss to project images and texts into a joint embedding space. Zheng *et al.* [8] proposed a dual-path CNN network and a instance loss for image-text retrieval. Zhang *et al.* [9] designed a cross-modal projection matching loss and a cross-modal projection classification loss to learn discriminative image-text embeddings. The above methods only learns global embeddings from images and texts. Recently, some advanced works [21], [25], [26] has focused on exploring the fine-grained interaction between modalities in the embedding space. Lee *et al.* [21] employed the bottom-up attention and bi-directional GRU network to get image region features and word features respectively, and presented a stacked cross attention to infer image-text similarity

by aligning image region and word features. Liu *et al.* [25] proposed a graph structured matching network to infer fine-grained correspondence between modalities. Different from them, all samples belong to a single category (person) for text-based person search, the fine-grained problem is the major challenge in distinguishing different persons. The core goal of the paper is to explore an effective embedding space in which the local fine-grained information of each modality can be effectively mined and the corresponding relationship between them.

C. Attention-Based Re-ID

Re-ID is a challenging task due to variations on viewpoints, low resolutions, illumination changes, unconstrained poses, occlusions, background clutter, heterogeneous modalities and so on. Attention mechanism can focus on important information related to task and suppress irrelevant information. In view of its advantages, many attention-based re-ID methods [3], [5], [27]–[31] have been proposed in recent years to overcome the above challenges. Yang *et al.* [27] designed the intra-attention and inter-attention modules to learn robust and discriminative human feature from global image and local parts, respectively. To introduce the global structural information, Zhang *et al.* [3] and Li *et al.* [5] explored the global scope relations for feature nodes at each location to learn attention for informative and discriminative feature learning. Some works employ the external clues as attention or to guide the attention learning. To eliminate the influence of background clutters on re-ID, Song *et al.* [29] designed a mask-guided contrastive attention model to guide the network to focus on the human body region, and proposes a region-level triplet loss to supervise the learning of the model. Different from the previous methods for mining discriminative visual feature, in order to alleviate the problem of information inequality between images and texts, we employ attention mechanism to guide the network to focus on the modality-shared image human body region and filter out the environmental factors while preserving the identity information.

III. ISANET FRAMEWORK

In this section, we provide an overall introduction to the proposed ISANet framework, as shown in Figure 2. Particularly, we first leverage CNN and RNN networks to extract visual and text representation respectively. After that, we feed the extracted image features to the image-specific information suppression module including relation-guide localization and channel attention filtration to eliminate the influence of image background and environmental factors. Then, the processed image features and text features are feed to the global and local encoding branches for global and local semantic alignment, respectively. Finally, the above modules are jointly optimized by identification loss, cross-modality triplet ranking loss, and identity-relevant content consistency loss to learn modality-aligned features for text-to-image retrieval.

A. Visual and Text Representations

Let $\mathcal{I} = \{\mathcal{I}_i\}_{i=1}^{N_x}$ and $\mathcal{T} = \{\mathcal{T}_i\}_{i=1}^{N_t}$ respectively denote image and text sets in a text-based person search database, where

N_x and N_t are the numbers of samples in each modality. The corresponding ground-truth label set $\mathcal{Y} = \{\mathcal{Y}_i\}_{i=1}^{N_y}$, where N_y is the number of identities. Given a text-image pair $(\mathcal{I}_i, \mathcal{T}_i)$, the goal is to encode it into a joint feature space to measure the similarity. For an image \mathcal{I}_i , we utilize a ResNet-50 [32] pretrained on ImageNet [33] with the final fully-connected layer removed as visual backbone to extract the visual feature map $\mathcal{F} \in \mathbb{R}^{C \times H \times W}$, where C denotes the number of feature channel with height H , and width W . Our goal is to achieve both global and local alignment between images and texts. To obtain the global and local features for each image, we introduce the global image branch F_{glb}^{image} and the local branch F_{loc} to generate a global visual feature $\mathcal{v}^g = F_{glb}^{image}(\mathcal{F}) \in \mathbb{R}^{d_g}$ and a set of local visual features $\{\mathcal{v}_1^l, \mathcal{v}_2^l, \dots, \mathcal{v}_K^l\} = F_{loc}(\mathcal{F}) \in \mathbb{R}^{K \times d_c}$, where K denote the number of local features.

For textual captions, we first create the vocabulary from the text database of the training set, only count some popular words whose appearance frequency more than 2 [15], and the size of vocabulary is V . After that, given a textual caption \mathcal{T}_i , we first encode each word in \mathcal{T}_i into a length- V one-hot vector \mathcal{v}_j . Then we transform the one-hot vector \mathcal{v}_j by a word embedding matrix $\mathcal{W}_e \in \mathbb{R}^{V \times d_e}$ into a d_e -dimensional word embedding \mathcal{w}_j :

$$\mathcal{w}_j = \mathcal{W}_e \mathcal{v}_j \quad (1)$$

The long short-term memory network (LSTM) as a special RNN has shown great capabilities in capturing the long-term dependencies among words. We adopt bi-directional LSTM (bi-LSTM) as text backbone to extract text features. After the embedding stage, all word embeddings $\{\mathcal{w}_1, \mathcal{w}_2, \dots, \mathcal{w}_L\}$ of the caption \mathcal{T}_i is feed into the bi-LSTM network in sequence to get the hidden states of forward and backward directions for each word. By averaging the hidden states of two directions to generate the corresponding contextual-aware text representation $\mathcal{e}_i \in \mathbb{R}^C$ for each word. All word representations for a caption are stacked as $\mathcal{E} = [\mathcal{e}_1, \mathcal{e}_2, \dots, \mathcal{e}_L] \in \mathbb{R}^{C \times L}$, where L is the number of words in each caption. It should be noted that the length of each caption is different. To ensure the consistency of caption length, we unify the length of the caption as L , select the first L words when the length is greater than L , and fill zero at the end of the caption when the length is less than L .

Similarly, in order to perform global and local alignment, we also obtain the global text feature $\mathcal{t}^g = F_{glb}^{text}(\mathcal{E}) \in \mathbb{R}^{d_g}$ and local text features $\{\mathcal{t}_1^l, \mathcal{t}_2^l, \dots, \mathcal{t}_K^l\} = F_{loc}(\mathcal{E}) \in \mathbb{R}^{K \times d_c}$ for each caption by the global text branch F_{glb}^{text} and the local branch F_{loc} . The details of the global branches F_{glb}^{image} , F_{glb}^{text} and the local branch F_{loc} are presented in the following.

B. Image-Specific Information Suppression

Considering the fact that the information contained in an image and a text is not equal, it is embodied in the following two aspects: First, the image is taken by camera at a relatively far distance from the person. The image not only contains the pedestrian, but also some surrounding background information (Figure 1(a)). Secondly, due to the task characteristics of re-ID, images are captured by multiple cameras at different times and places. Due to the differences of camera parameters and

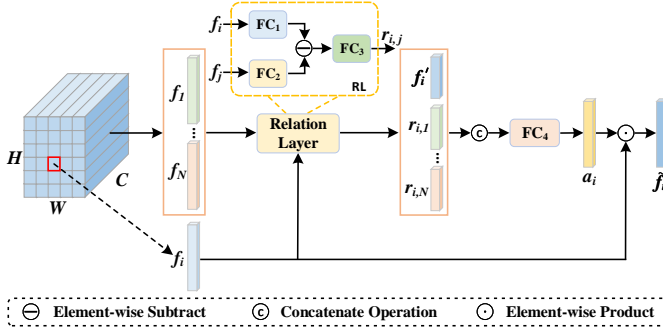


Fig. 3. The architecture of relation-guide localization (RGL) module.

environment (lighting conditions, weather, viewpoint, etc.), the captured images contain some environmental factors, which lead to great intra-class variances, that is, multiple images of the same person are very different (Figure 1(b)).

Compared with images, texts are clean, and most of them are descriptions of pedestrian appearance information. Therefore, the background information and environmental factors in the image are noise for text, which increases the modality gap between images and texts. In order to solve this problem, we propose an image-specific information suppression module, which includes two sub-modules, relation-guide localization (RGL) and channel attention calibration (CAF), to deal with background and environmental factors respectively, and alleviate the information inequality between images and texts. The solution of this problem can effectively narrow the gap between modalities and achieve the information alignment.

Relation-Guide Localization (RGL). The attention mechanism is widely used in various tasks due to its advantages in strengthening discriminative features and suppressing irrelevant one, which matches well our purpose. Some works [3], [5] has proved that the relations among spatial positions in the image provide clustering-like information, which is helpful for the semantic understanding of image. Therefore, a relation-guide localization module is introduced to guide attention learning through the relations among spatial positions, so that it can suppress background and highlight the image pedestrian region corresponding to the text description, as shown in Figure 3.

It is crucial how to measure the relation between features effectively. The most common way is to utilize the Euclidean or cosine distance to compute the relational scalar between different features, which can indicate the degree of correlation between them while lacks the detailed correspondence. Different from them, we capture more detailed associations among spatial positions by computing a relation vector instead of a relation scalar. The relation function between vectors $\mathbf{x} \in \mathbb{R}^d$ and $\mathbf{y} \in \mathbb{R}^d$ is formulate as:

$$r(\mathbf{x}, \mathbf{y}; \mathbf{W}, \mathbf{W}_\theta, \mathbf{W}_\phi) = \mathbf{W}(\mathbf{x}_\theta - \mathbf{y}_\phi) \quad (2)$$

where $\mathbf{W} \in \mathbb{R}^{r_2 \times \frac{d}{r_1}}$ denotes a learnable parameter matrix obtained by a fully connected (FC) layer followed by a batch normalization (BN) and a rectified linear unit (ReLU) to get a r_2 -dimensional relation vector. $\mathbf{x}_\theta = \text{ReLU}(\text{BN}(\mathbf{W}_\theta \mathbf{x}))$ and $\mathbf{y}_\phi = \text{ReLU}(\text{BN}(\mathbf{W}_\phi \mathbf{y}))$. $\mathbf{W}_\theta, \mathbf{W}_\phi \in \mathbb{R}^{\frac{d}{r_1} \times d}$ reduce the

feature vector dimension with factor r_1 .

With the visual feature map $\mathbf{F} \in \mathbb{R}^{C \times H \times W}$ from the visual backbone, we calculate the relationship between each spatial location and all spatial locations to obtain the attention score of each spatial location. Specifically, for a feature vector $\mathbf{f}_i \in \mathbb{R}^C$ at i -th position, we compute the relation between it and all $N (N = H \times W)$ positions to get N relation vectors. Then the N relation vectors are concatenated to denote the global relation vector $\mathbf{r}_i \in \mathbb{R}^{\frac{NC}{r_1}}$ at i -th position:

$$\mathbf{r}_i = \text{Concat}([\mathbf{r}_{i,1}, \mathbf{r}_{i,2}, \dots, \mathbf{r}_{i,N}]) \quad (3)$$

$$\mathbf{r}_{i,j} = r(\mathbf{f}_i, \mathbf{f}_j, \mathbf{W}, \mathbf{W}_\theta, \mathbf{W}_\phi), (1 \leq j \leq N) \quad (4)$$

To obtain the attention at the i -th position, we combine the visual feature \mathbf{f}_i with its corresponding global relation vector \mathbf{r}_i to generate the attention by a projection function implemented by FC layer followed by BN and Sigmoid function:

$$\mathbf{a}_i = \text{Sigmoid}(\text{BN}(\mathbf{W}_a[\mathbf{f}_i, \mathbf{r}_i])) \quad (5)$$

where $\mathbf{W}_a \in \mathbb{R}^{C \times (\frac{N}{r_1}+1)C}$ and $\mathbf{a}_i \in \mathbb{R}^C$. For all positions, we get an attention map $\mathbf{A} \in \mathbb{R}^{C \times H \times W}$. Finally, the attention map \mathbf{A} and the visual feature map \mathbf{F} perform element-wise product to get the enhanced feature map $\tilde{\mathbf{F}}$.

Channel Attention Filtration (CAF). Due to the existence of environmental factors in the image, it not only enlarges the inter-modal gap, but also causes huge intra-class variations within images. To eliminate the influence of environmental factors, we introduce a channel attention filtration module, as shown in Figure 4.

A lot of works [34]–[36] show that Instance Normalization (IN) can effectively reduce the discrepancy among instances by filtering out some instance-specific style information. However, directly applying IN may inevitably remove some identity-relevant information, thereby damaging discrimination capability of features. To avoid the problem, we further mine the identity-relevant information from the IN removed information after instance normalization. Specifically, we first perform Instance Normalization on the visual feature $\tilde{\mathbf{F}}$ processed by RGL to remove the style information.

$$\tilde{\mathbf{F}}_{IN} = \text{IN}(\tilde{\mathbf{F}}) = \gamma \left(\frac{\tilde{\mathbf{F}} - \mu(\tilde{\mathbf{F}})}{\sigma(\tilde{\mathbf{F}})} \right) + \beta \quad (6)$$

where $\mu(\cdot)$ and $\sigma(\cdot)$ denote the mean and standard-deviation, $\gamma, \beta \in \mathbb{R}^C$ are parameters learned from data. Next, we restore the identity-relevant information by distilling it from the IN removed information. The IN removed information is defined as:

$$\mathbf{R} = \tilde{\mathbf{F}} - \tilde{\mathbf{F}}_{IN} \quad (7)$$

With the IN removed information \mathbf{R} , we mine the identity-relevant information from it through channel attention, and then add it to the instance normalized feature.

$$\hat{\mathbf{F}} = \tilde{\mathbf{F}}_{IN} + \mathbf{w}_C \odot \mathbf{R} + \tilde{\mathbf{F}} \quad (8)$$

where $\mathbf{w}_C \in \mathbb{R}^C$ is the channel-wise attention weight indicating the identity-relevant channels, which is generate in the same

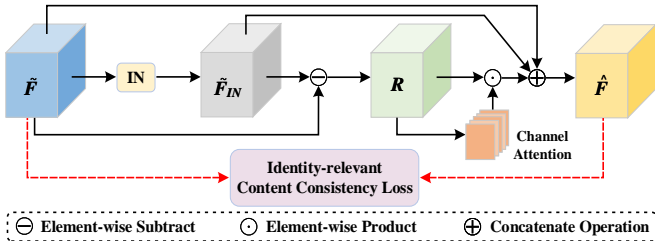


Fig. 4. The architecture of channel attention filtration (CAF) module.

way as [37]. With the channel attention filtration module, we expect that the output feature can fully retain effective identity information while discarding redundant noise information. To further ensure the capability, we introduce an identity-relevant content consistency loss. See section F for details.

After the aforementioned text encoding and image encoding, localization and filtration, the problem of information inequality between images and texts is alleviated, and obtain the text feature map $\hat{\mathbf{E}} \in \mathbb{R}^{C \times L \times 1}$ and image feature map $\hat{\mathbf{F}} \in \mathbb{R}^{C \times H \times W}$. Although $\hat{\mathbf{F}}$ and $\hat{\mathbf{E}}$ achieve the alignment at the information level, the image is spatially structured and the text is orderless. It is not feasible to directly compare the two types of features since they are not well-aligned at the semantic level. For this reason, we perform global and local semantic alignment between images and texts in the following, respectively.

C. Implicit Local Alignment

Local-level alignment by mining fine-grained information for images and texts are essential for text-based person search. The expression for pedestrians can have different forms, such as image, text, voice and so on, but the semantic information they contain is the same. Therefore, we believe that there are a group of latent semantic topics in a shared semantic space, which can completely express the semantic information of pedestrians, and are shared by different modalities. Motivated by this spirit, we propose an implicit local semantic alignment module to adaptively select and aggregate the image and text features to the same topics, and obtain multiple locally aligned image and text features.

Suppose there is a set of semantic topic centers $\{c_1, c_2, \dots, c_K\}$ in a shared semantic space, where K denotes the number of centers, and $c_i \in \mathbb{R}^{d_c}$, d_c is the dimension of shared semantic space. These centers can be learned jointly with the whole network. Then we assign image and text features to corresponding topic centers by calculating the similarities between features and centers in the same way as Eq. (2). We first depict the assignment on visual feature map in details, and then roughly describe that on text feature map since this operation is the same on two kinds of feature maps. Given the visual feature map $\hat{\mathbf{F}} \in \mathbb{R}^{C \times H \times W}$, first project it into the shared semantic space by a 1×1 convolution layer $\mathbf{W}_s \in \mathbb{R}^{d_c \times C}$ after L2-normalization:

$$\mathbf{Z}^{image} = \mathbf{W}_s \text{Normalize}(\hat{\mathbf{F}}) \quad (9)$$

where $\mathbf{Z}^{image} \in \mathbb{R}^{d_c \times H \times W}$. Next we compute assignments on the corresponding centers for each spatial position. Specifically,

for the feature vector $\mathbf{z}_i^{image} \in \mathbb{R}^{d_c}$ at i -th position in \mathbf{Z}^{image} , its assignment to j -th topic center c_j can be generated in the same way as Eq. (2) as follow:

$$\mathbf{a}_{i,j}^{image} = r(\mathbf{z}_i^{image}, c_j, \mathbf{W}^l, \mathbf{W}_\theta^l, \mathbf{W}_\phi^l) \quad (10)$$

where $\mathbf{W}^l \in \mathbb{R}^{d_c \times \frac{d_c}{r_3}}$, and $\mathbf{W}_\theta^l, \mathbf{W}_\phi^l \in \mathbb{R}^{\frac{d_c}{r_3} \times d_c}$ are all learnable parameter matrices. Then the aggregated local image feature for each center can be obtained,

$$\mathbf{v}_j^l = \sum_{i=1}^N \mathbf{a}_{i,j}^{image} \mathbf{z}_i^{image} \quad (11)$$

where $N = H \times W$ denotes the number of spatial position. Thus, we can generate a set of aggregated local image feature $\{\mathbf{v}_1^l, \mathbf{v}_2^l, \dots, \mathbf{v}_K^l\}$ for all semantic topic centers. Similarly, we can also generate a set of aggregated local text feature $\{\mathbf{t}_1^l, \mathbf{t}_2^l, \dots, \mathbf{t}_K^l\}$ in the same way using the shared semantic topic centers.

$$\mathbf{Z}^{text} = \mathbf{W}_s \text{Normalize}(\hat{\mathbf{E}}) \quad (12)$$

$$\mathbf{a}_{i,j}^{text} = r(\mathbf{z}_i^{text}, c_j, \mathbf{W}^l, \mathbf{W}_\theta^l, \mathbf{W}_\phi^l) \quad (13)$$

$$\mathbf{t}_j^l = \sum_{i=1}^L \mathbf{a}_{i,j}^{text} \mathbf{z}_i^{text} \quad (14)$$

where L denotes the length of caption, $\mathbf{z}_i^{text} \in \mathbb{R}^{d_c}$ is the feature vector of i -th word in \mathbf{Z}^{text} . Finally, we respectively concatenate all local image and text feature to get the output feature $\mathbf{v}^l \in \mathbb{R}^{Kd_c}$ and $\mathbf{t}^l \in \mathbb{R}^{Kd_c}$, which are aligned effectively since the learned local features for images and texts share the same semantic topic centers.

D. Global Alignment

Moreover, we also introduce global alignment since the global features contain more comprehensive information and complementary to local features. For visual feature map $\hat{\mathbf{F}} \in \mathbb{R}^{C \times H \times W}$, we first project it into a joint semantic embedding space through a fully connected layer \mathbf{W}_g^{image} . Because only part of the image region is related to the text description, considering that the global max-pooling layer can mine salient information and filter out noise, thus perform global max-pooling (GMP) to obtain the global visual feature.

$$\mathbf{v}^g = \text{GMP}(\mathbf{W}_g^{image} \hat{\mathbf{F}}) \quad (15)$$

For text feature map $\hat{\mathbf{E}} \in \mathbb{R}^{C \times L \times 1}$, first perform global max-pooling to get feature vector. Then we also project the obtained feature vector into the joint semantic embedding space by a fully connected layer \mathbf{W}_g^{text} to obtain the global text feature.

$$\mathbf{t}^g = \mathbf{W}_g^{text} \text{GMP}(\hat{\mathbf{E}}) \quad (16)$$

where $\mathbf{v}^g, \mathbf{t}^g \in \mathbb{R}^{d_g}$.

E. Training Loss and Inference

Once the global and local features for images and texts have been obtained by the proposed model, we train the model

with identification loss, cross-modality triplet ranking loss, and identity-relevant content consistency loss. The detailed descriptions of each loss are presented in the following.

Identification Loss. We adopt the identification loss to classify persons into different groups by their identities, which ensures the identity-level matching. Specifically, the cross-entropy loss is imposed on the global feature and each of the K local features. Therefore, the total identification loss \mathcal{L}_{id} is:

$$\mathcal{L}_{id} = \mathcal{L}_{id}^g + \sum_{k=1}^K \mathcal{L}_{id}^{l_k} \quad (17)$$

Cross-Modality Triplet Ranking Loss. We employ the common cross-modality bi-directional dual-constrained triplet ranking loss to supervise the modality-shared global and local feature learning. In addition, we also introduce text descriptions of other images with the same identity as [15] as weak supervision signal to overcome the intra-class variance in the text.

$$\begin{aligned} \mathcal{L}_{rank}^z = & \max(\alpha_1 - S(\mathbf{v}_p^z, \mathbf{t}_p^z) + S(\mathbf{v}_n^z, \mathbf{t}_n^z), 0) \\ & + \max(\alpha_1 - S(\mathbf{v}_p^z, \mathbf{t}_p^z) + S(\mathbf{v}_n^z, \mathbf{t}_p^z), 0) \\ & + \lambda_1 \max(\alpha_2 - S(\mathbf{v}_p^z, \bar{\mathbf{t}}_p^z) + S(\mathbf{v}_p^z, \mathbf{t}_n^z), 0) \\ & + \lambda_1 \max(\alpha_2 - S(\mathbf{v}_p^z, \bar{\mathbf{t}}_p^z) + S(\mathbf{v}_n^z, \bar{\mathbf{t}}_p^z), 0) \end{aligned} \quad (18)$$

where \mathbf{v}^z and \mathbf{t}^z ($z = g, l$) denote the global or local feature for image and text, respectively. $\bar{\mathbf{t}}^z$ denotes the text feature corresponding to another image with the same identity as \mathbf{v}^z . $(\mathbf{v}_p^z, \mathbf{t}_p^z)$ denotes the matched image-text pairs, and $(\mathbf{v}_p^z, \mathbf{t}_n^z), (\mathbf{v}_n^z, \mathbf{t}_p^z)$ denote the mismatched pairs. α_1 and α_2 indicate the margins, and the setting strategy of α_2 keeps same with [15], λ_1 is hyper-parameters.

$$\mathcal{L}_{rank} = \mathcal{L}_{rank}^g + \mathcal{L}_{rank}^l \quad (19)$$

Identity-relevant Content Consistency Loss is introduced to ensure that CAF module can fully retain effective identity information while discarding redundant noise information. Specifically, we hope that the identity-relevant information can retain consistent before and after passing through CAF module, while only filter out noise information. A triplet loss is adapted to achieve the goal.

$$\begin{aligned} \mathcal{L}_{cons} = & \max(\alpha_3 - S(\tilde{\mathbf{f}}, \hat{\mathbf{f}}) + S(\tilde{\mathbf{f}}, \hat{\mathbf{f}}_n), 0) \\ & + \max(\alpha_3 - S(\tilde{\mathbf{f}}, \hat{\mathbf{f}}) + S(\tilde{\mathbf{f}}_n, \hat{\mathbf{f}}), 0) \end{aligned} \quad (20)$$

where $\tilde{\mathbf{f}} = GAP(\tilde{\mathbf{F}})$, $\hat{\mathbf{f}} = GAP(\hat{\mathbf{F}})$ respectively represent the feature vectors before and after \mathbf{F} pass through CAF module, and $GAP(\cdot)$ denotes the global average pooling. \mathbf{f}_n , $\hat{\mathbf{f}}_n$ denote the hardest negative sample for \mathbf{F} before and after through CAF module in a mini-batch, respectively. α_3 is the corresponding margin. $S(\cdot, \cdot)$ denotes the similarity function. The loss retains the identity information by pulling the distance between $\tilde{\mathbf{f}}$ and $\hat{\mathbf{f}}$ as close as possible, and ensures the discrimination ability of features by pulling distances between $\tilde{\mathbf{f}}$ and $\hat{\mathbf{f}}_n$, $\tilde{\mathbf{f}}_n$ and $\hat{\mathbf{f}}$ as far as possible.

Finally, the total loss \mathcal{L}_{total} is utilized to train our model in an end-to-end manner as follow:

$$\mathcal{L}_{total} = \mathcal{L}_{id} + \mathcal{L}_{rank} + \lambda_2 \mathcal{L}_{cons} \quad (21)$$

where λ_2 is hype-parameters to balance the contributions of individual loss terms.

During the testing stage, for each text query and image gallery, we respectively compute the similarity scores S^g, S^l of global features and local features between them by cosine similarity function. Then we rank the similarity score $S = S^g + S^l$ to retrieve the person images from image gallery based on the text query.

IV. EXPERIMENTS

In this section, we conduct extensive experiments on two text-based person search databases to verify the effectiveness and superiority of the proposed method. First, we introduce two public large-scale databases, the implementation and training details of the proposed model. Then we compare our method with the state-of-the-art methods on two databases. Finally, some ablation studies were shown to prove the effectiveness of each component.

A. Experiment Settings

1) **Datasets:** **CUHK-PEDES** [7] is the most commonly used large-scale benchmark database for text-based person search. It provides 40,206 images and 80,412 text descriptions of 13,003 persons collected from some existing image-based Re-ID databases, wherein each image is manually annotated with 2 text descriptions, and each text describes important details of the corresponding images, with an average length of not less than 23 words. The whole database constitutes a vocabulary with a total of 9408 unique words. To perform a fair comparison with existing methods, we follow the official data split protocol in [7]. Specifically, 34,054 images of 11,003 persons and corresponding 68,108 text descriptions are used as the training set. The remaining 2000 persons are equally divided into the validation set and the testing set, in which the validation set contains 3,078 images and 6,156 text descriptions, while the testing set contains 3,074 images and 6,148 text descriptions.

ICFG-PEDES is new large-scale database recently released by [15], which contains more identity-centric and fine-grained text descriptions than CUHK-PEDES. The database contains 54,522 images of 4,102 persons collected from the MSMT17 [38] database, each of which corresponds to a text description with an average length of 37 words. The vocabulary contains 5554 unique words. Following the data split protocol in [15], the database is divided into the training set and the testing set, in which the training set contains 34674 image-text pairs of 3102 persons, while the testing set consists of 19848 image-text pairs of the remaining 1000 persons. For both databases, the Rank-K ($K=1, 5, 10$, higher is better) is adopted to evaluate the performance of different methods.

2) **Implementation Details:** For images, we use ResNet-50 [32] pre-trained on imageNet [33] as image backbone, and make minor modifications: remove the average pooling layer and fully connected layer, and set the stride of the last convolution layer to 1 for larger feature map. All images are resized to 384×128 before being fed into the image backbone, followed by horizontal flipping for data augmentation. For texts, Bi-LSTM is used as the text backbone, and likewise, the text length is unified

TABLE I
PERFORMANCE COMPARISON WITH STATE-OF-THE-ART METHODS ON CUHK-PEDES. RANK-1, RANK-5, AND RANK-10 ARE LISTED. '-' DENOTES THAT NO REPORTED RESULT IS AVAILABLE. "G" INDICATES THAT THE METHODS ONLY PERFORM GLOBAL ALIGNMENT. "L" INDICATES THAT THE METHODS ALSO PERFORM LOCAL ALIGNMENT.

Methods	Type	Ref	Rank-1	Rank-5	Rank-10
GNA-RNN [7]	G	CVPR17	19.05	-	53.64
IATV [17]	G	ICCV17	25.94	-	60.48
Dual Path [8]	G	TOMM20	44.40	66.26	75.07
CMPM/C [9]	G	ECCV18	49.37	-	79.27
MCCL [39]	G	ICASSP19	50.58	-	79.06
A-GANet [40]	G	MM19	53.14	74.03	81.95
TIMAM [41]	G	ICCV19	54.51	77.56	84.78
CMKA [10]	G	TIP21	54.69	73.65	81.86
TDE [42]	G	MM20	55.25	77.46	84.56
VTA [43]	G	arXiv19	55.32	77.00	84.26
LapsCore [23]	G	ICCV21	57.00	-	85.62
PWM+ATH [44]	L	WACV18	27.14	49.45	61.02
GLA [18]	L	ECCV18	43.58	66.93	76.26
MIA [19]	L	TIP20	53.10	75.00	82.90
PMA [20]	L	AAAI20	53.81	73.54	81.23
SCAN [21]	L	ECCV18	55.86	75.97	83.69
ViTAA [11]	L	ECCV20	55.97	75.84	83.52
IMG-Net [45]	L	JEI20	56.48	76.89	85.01
CMAAM [12]	L	WACV20	56.68	77.18	84.86
HGAN [22]	L	MM20	59.00	79.49	86.62
NAFS [13]	L	arXiv21	59.94	79.86	86.70
DSSL [14]	L	MM21	59.98	80.41	87.56
MGEL [46]	L	IJCAI21	60.27	80.01	86.74
SSAN [15]	L	arXiv21	61.37	80.15	86.73
AXM-Net (w2v) [47]	L	AAAI22	61.90	79.40	85.75
Ours	L	-	63.92	82.15	87.69

to $L = 100$ before all texts is sent into the text backbone. The classifier $C(\cdot)$ is implemented by a fully-connected layer. The dimensions of some parameters in the proposed model are set as $H = 24$, $W = 8$, $C = 2048$, $d_e = 512$, $d_g = 2048$ and $d_c = 512$. The scale factors r_1 , r_2 and r_3 are set to 32, 256 and 4, respectively. The size of the vocabulary in the training set varies for different databases, with CUHK-PEDES set to $V = 5000$ and ICFG-PEDES set to $V = 3000$.

In the training process, we use Adam as the optimizer to optimize the model. The learning rate for the visual backbone is initialized to 0.001, and for the rest of the network layers are initialized to 0.01, which decays at the 30th and 50th epoch with a decay factor of 0.1. For the convenience of training, we first introduce the linear warm-up strategy to optimize the model in the first 10 epochs. The model was trained for a total of 70 epoch with the batch-size of 64. The cross-modality triplet ranking loss margin α_1 is set to 0.2. The identity-relevant content consistence loss margin α_2 is also set to 0.2. The hyper-parameters λ_1 and λ_2 are set to 0.1 and 1. We implement the proposed model with PyTorch and train it on a single RTX3090 GPU.

B. Comparison with State-of-the-art

In this section, we evaluate our method by comparing with the state-of-the-art (SOTA) methods on two public

databases, as shown in Tables I and II. Our method consistently improve the state-of-the-art on all of these two public databases. The compared SOTAs can be divided into two groups: (1) global-matching methods, including GNA-RNN [7], IATV [17], Dual Path [8], CMPM/C [9], MCCL [39], A-GANet [40], TIMAM [41], CMKA [10], TDE [42], VTA [43], LapsCore [23], and (2) local-matching methods, including PWM+ATH [44], GLA [18], MIA [19], PMA [20], SCAN [21], ViTAA [11], IMG-Net [45], CMAAM [12], HGAN [22], NAFS [13], DSSL [14], MGEL [46], SSAN [15], AXM-Net [47].

1) *Results on CUHK-PEDES*: We first evaluate the proposed method on the most common benchmark, **CUHK-PEDES**, as shown in Table I. It can be seen that the methods based on local alignment have taken the mainstream and achieved superior performance in recent years. Among the above-mentioned local-matching methods, PWM+ATH, MIA, PMA, SCAN, HGAN, NAFS, DSSL and AXM-Net align images and texts by introducing an attention mechanism for complex cross-modal interactions. In addition, the existing methods obtain local features by hand-crafted split or external tools. Our method implicitly obtains locally aligned features directly from the original feature map without any additional supervision and complex inter-modal interactions, which is simpler and more efficient. The

proposed ISANet also surpasses the existing SOTAs by a large margin and achieves new state-of-the-art results. Specifically, our method achieves 63.92%, 82.15% and 87.69% of Rank-1, Rank-5 and Rank-10 accuracies respectively, 2.02%, 2.75% and 1.94% improvement on the Rank-1, Rank-5 and Rank-10 are obtain over the best SOTA AXM-Net [47].

2) *Results on ICFG-PEDES*: To prove the generality of the proposed ISANet, we also evaluate the performance on another newly released large-scale database, **ICFG-PEDES**. The comparison results are shown in Table II. There are only a few methods to compare since the database is up-to-date. Similar to the results on CUHK-PEDES, the proposed method outperforms all existing methods reported on ICFG-PEDES by a large margin in all metrics, achieves Rank-1 of 57.73%, Rank-5 of 75.42% and Rank-10 of 81.72%, significantly surpasses the best SOTA SSAN [15] by 3.50% on Rank-1, 2.79% on Rank-5, 2.19% on Rank-10.

TABLE II
PERFORMANCE COMPARISON WITH STATE-OF-THE-ART METHODS ON ICFG-PEDES. RANK-1, RANK-5, AND RANK-10 ARE LISTED. ‘-’ DENOTES THAT NO REPORTED RESULT IS AVAILABLE.

Methods	Ref	Rank-1	Rank-5	Rank-10
Dual Path [8]	TOMM20	38.99	59.44	68.41
CMPM/C [9]	ECCV18	43.51	65.44	74.26
MIA [19]	TIP20	46.49	67.14	75.18
SCAN [21]	ECCV18	50.05	69.65	77.21
ViTAA [11]	ECCV20	50.98	68.79	75.78
SSAN [15]	arXiv21	54.23	72.63	79.53
Ours	-	57.73	75.42	81.72

The above results prove the superiority and generality of the proposed ISANet for text-based person search. It benefits from its ability in image-specific information suppression and implicit aligned local feature learning of the proposed model, effectively narrowing the information and semantic gap between images and texts, which will be further demonstrated in the next section.

C. Ablation Studies

In this section, we investigate the contribution of each module in the proposed ISANet and the effect of important parameter on CUHK-PEDES, including global alignment (GA), implicit local alignment (ILA), image-specific information suppression module (including relation-guide localization (RGL) and channel attention filtration (CAF)), and the number K of topic centers. The Rank-1, Rank-5, Rank-10 accuracies (%) are reported.

1) *Effectiveness of Components*: In order to clearly illustrate the effectiveness of each component, we add them into the model one by one. The experimental results are shown in Table III. We adopt SSAN [15] as Baseline by removing its part-level feature extraction branch, and modify the stride of the last convolution layer of image backbone (ResNet-50) to 1, then train Baseline by the same training strategy as ours, and everything else is consistent with SSAN. The first row shows the results of Baseline.

GA represents replacing the shared 1×1 convolution in Baseline as our global alignment module, the result is shown

in the second line. Compared with Baseline, GA improves rank-1, rank-5 and rank-10 by 2.35% and 2.23% and 1.68% respectively. When ILA module is added to Baseline, the Rank-1, Rank-5, and Rank-10 accuracies are significantly improved by 3.88%, 2.93%, and 2.47% over Baseline, which demonstrates that this method of implicitly learning locally aligned features by a set of modality-shared semantic topic centers can effectively model the local fine-grained correspondence between images and texts, and narrow the semantic gap across modalities. The joint deployment of GA and ILA can further improve performance, the rank-1 accuracy on CUHK-PEDES achieving 62.43%, which has surpassed all SOTAs in Table I, further proving the superiority of our method. Moreover, the result also demonstrates that GA and ILA can work cooperatively with each other to align images and texts from different granularities.

Although the combination of GA and ILA has achieved the SOTA results, RGL and CAF can further improve the rank-1 accuracy by 1.12% and 1.22% respectively based on the above results, since RGL and CAF consider the influence of image-specific information, especially image background and environmental factors, and alleviates the information inequality between modalities. The joint deployment of RGL and CAF can further improve performance, and achieve the best. All the above results show that each module in the proposed ISANet can play an positive role effectively in alleviating modality gap.

2) *Effectiveness of Image-Specific Information Suppression*: The attention mechanism plays an vital role in image-specific information suppression module. In order to prove the advantages of RGL and CAF in suppressing image-specific information, we conduct a series of comparative experiments, including directly using instance normalization (IN) to eliminate environmental factors, removing identity-relevant content consistence loss L_{cons} designed in CAF module, and replacing RGL with some existing attention methods (including CBAM [48], Non-Local [49], RGA [3]). A→B means replacing A with B, leaving the rest unchanged. The results are shown in Table IV.

When replacing CAF with IN, although the environmental factors are filtered out, some discriminative identity-relevant information is also lost. Compared with ISANet, the Rank-1 accuracy drops by 1.66%. CAF utilizes channel attention to restitute useful identity information from the IN removed information, which effectively alleviates the identity-relevant information loss problem. At the same time, CAF designs a identity-relevant content consistency loss to promote information restitution and improve feature discrimination, and the Rank-1 accuracy is improved by nearly 0.5%. Moreover, we also replace RGL with some existing attention methods, and the performance is more or less degraded, which proves that RGL mines global structural information guided by relations to help understand image semantics, suppress background more effectively, and the modality-shared human body region is focused on under the supervision of the cross-modal ranking loss.

3) *Different Aggregation Strategy*: In the proposed implicit local alignment (ILA) module, image and text features are aligned by adaptively aggregating them into a set of shared semantic topic centers, in which feature aggregation strategy is

TABLE III
ABLATION STUDY ON DIFFERENT COMPONENTS OF OUR PROPOSED MODEL ON CUHK-PEDES.

Method	GA	ILA	RGL	CAF	Rank-1	Rank-5	Rank-10
Baseline					57.80	77.32	84.45
GA	✓				60.15	79.55	86.13
ILA		✓			61.68	80.25	86.92
GA+ILA	✓	✓			62.43	81.14	87.35
GA+ILA+RGL	✓	✓	✓		63.55	81.56	87.61
GA+ILA+CAF	✓	✓		✓	63.65	81.22	87.54
GA+ILA+RGL+CAF (Ours)	✓	✓	✓	✓	63.92	82.15	87.69

TABLE IV
ABLATION STUDY OF IMAGE-SPECIFIC INFORMATION SUPPRESSION
MODULE ON CUHK-PEDES.

Method	Rank-1	Rank-5	Rank-10
ISANet	63.92	82.15	87.69
CAF→IN	62.26	80.54	87.02
CAF (w/o \mathcal{L}_{cons})	63.47	81.38	87.91
RGL→CBAM [48]	63.03	81.11	87.90
RGL→Non-Local [49]	62.09	81.06	87.61
RGL→RAG [3]	63.17	81.47	87.56

TABLE V
EFFECTS OF DIFFERENT FEATURE AGGREGATION ON CUHK-PEDES. 'IP'
REPRESENTS INNER-PRODUCT OPERATION.

Method	Rank-1	Rank-5	Rank-10
NetVLAD [50]	61.09	80.99	86.81
ILA (IP)	61.19	80.04	87.04
ILA (Ours)	63.92	82.15	87.69

crucial. We compared different aggregation strategies, as shown in Table V. NetVLAD [50] is a classic feature aggregation method. ILA (IP) means that the assignment to each center is calculated by inner product (IP) operation. But IP can only indicate to what extent two features are similar, and our method uses a relation function to calculate the detailed correspondence between the features. The results show that our aggregation strategy achieves the best results, 2.83% and 2.73% higher than the other two strategies respectively, since this detailed correspondence can provide more accurate assignments when aggregating features to each semantic center.

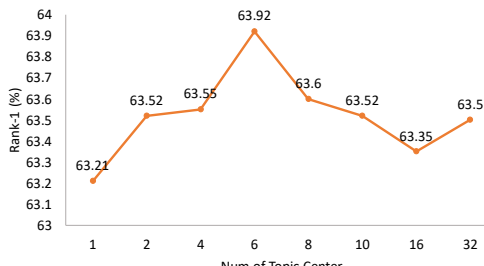


Fig. 5. Effect of different number of semantic topic centers.

4) *Number of Topic Centers*: Intuitively, K determines the granularity of the local feature. We choose the most appropriate K in the range from 1 to 32, as illustrated in Figure 5. The results show that if the value of K is too small, the granularity of the obtained local features is very small, and it is impossible to establish fine-grained correspondence between modalities. When $K=1$, the learned features represent a global one. As K increases, Rank-1 accuracy gradually increases, but begins to decrease after it is greater than 6. We believe that too large granularity will lead to semantic fragmentation and severely destroy the semantics of images and texts. When $K=6$, our proposed method achieves the best results.

5) *Qualitative Results*: Figure 6 shows the top-7 retrieval results of our method and baseline for the given text query. It can be seen from the figure that our method achieves more accurate retrieval results. For some cases where baseline fails, our method can also find the correct result at top-3. For a given text query, although there are some incorrect results in the top-7 retrieved images, the semantic attributes described in the text query are there in almost retrieval results, which shows that our method realizes modality alignment between images and texts, and can effectively mine the detailed correspondence between them. Moreover, from the results, we can also find that the retrieval accuracy is dominated by color information to a great extent for text-image retrieval. However, as mentioned earlier, images are easily affected by the environment, which leads to the distortion of semantic information, so it is not reliable to take color information as the leading retrieval clue. If we can mine deeper semantic information, it will greatly improve the accuracy and robustness of existing methods, which will be our future work.

V. CONCLUSION

In this paper, we propose an efficient joint information and semantic alignment network, termed ISANet, to alleviate the modality discrepancy between images and texts for text-based person search. Our method aims to both alleviate the information inequality between modalities and implicitly learn the local fine-grained correspondence between images and texts. Specifically, ISANet firstly employs Image-Specific Information Suppression module to alleviate information inequality problem between modalities, in which Relation-Guide Localization sub-module models global relation information to help localize the human body region, and Channel Attention Filtration sub-module applies instance normalization and channel attention to



Fig. 6. Comparison of top-7 retrieval results on CUHK-PEDES between our method and the baseline for the same query texts. The retrieval results from top-1 to top-7 are shown from left to right. The correct results are marked by red rectangles.

eliminate environmental factors while preserving the identity information. Then, in the Implicit Local Alignment module, image and text features are adaptively aggregated into a set of shared semantic topic centers to implicitly learn locally aligned features without any extra supervised information and complex cross-modal interactions. Finally, a Global Alignment module is introduced to provide a global cross-modal measurement that is complementary to the local perspective. We optimize the proposed ISANet in an end-to-end manner. Both qualitative and quantitative experimental results, as well as extensive ablation studies prove the superiority and effectiveness of ISANet.

REFERENCES

- [1] L. Zhang, G. Du, F. Liu, H. Tu, and X. Shu, “Global-local multiple granularity learning for cross-modality visible-infrared person reidentification,” *IEEE Transactions on Neural Networks and Learning Systems*, pp. 1–11, 2021.
- [2] H. Li, S. Yan, Z. Yu, and D. Tao, “Attribute-identity embedding and self-supervised learning for scalable person re-identification,” *IEEE Transactions on Circuits and Systems for Video Technology*, vol. 30, no. 10, pp. 3472–3485, 2019.
- [3] Z. Zhang, C. Lan, W. Zeng, X. Jin, and Z. Chen, “Relation-aware global attention for person re-identification,” in *IEEE/CVF Conference on Computer Vision and Pattern Recognition, CVPR*, 2020, pp. 3183–3192.
- [4] R. Hou, H. Chang, B. Ma, R. Huang, and S. Shan, “Bicnet-tks: Learning efficient spatial-temporal representation for video person re-identification,” in *IEEE Conference on Computer Vision and Pattern Recognition, CVPR*, 2021, pp. 2014–2023.
- [5] X. Li, W. Zhou, Y. Zhou, and H. Li, “Relation-guided spatial attention and temporal refinement for video-based person re-identification,” in *The Thirty-Fourth AAAI Conference on Artificial Intelligence, AAAI*, 2020, pp. 11434–11441.
- [6] W. Zhang, X. He, W. Lu, H. Qiao, and Y. Li, “Feature aggregation with reinforcement learning for video-based person re-identification,” *IEEE Transactions on Neural Networks and Learning Systems*, vol. 30, no. 12, pp. 3847–3852, 2019.
- [7] S. Li, T. Xiao, H. Li, B. Zhou, D. Yue, and X. Wang, “Person search with natural language description,” in *IEEE Conference on Computer Vision and Pattern Recognition, CVPR*, 2017, pp. 5187–5196.
- [8] Z. Zheng, L. Zheng, M. Garrett, Y. Yang, M. Xu, and Y. Shen, “Dual-path convolutional image-text embeddings with instance loss,” *ACM Transactions on Multimedia Computing, Communications, and Applications (TOMM)*, vol. 16, no. 2, pp. 51:1–51:23, 2020.
- [9] Y. Zhang and H. Lu, “Deep cross-modal projection learning for image-text matching,” in *European Conference on Computer Vision, ECCV*, 2018, pp. 707–723.
- [10] Y. Chen, R. Huang, H. Chang, C. Tan, T. Xue, and B. Ma, “Cross-modal knowledge adaptation for language-based person search,” *IEEE Transactions on Image Processing*, vol. 30, pp. 4057–4069, 2021.
- [11] Z. Wang, Z. Fang, J. Wang, and Y. Yang, “Vitaa: Visual-textual attributes alignment in person search by natural language,” in *European Conference on Computer Vision, ECCV*, 2020, pp. 402–420.
- [12] S. Aggarwal, R. V. Babu, and A. Chakraborty, “Text-based person search via attribute-aided matching,” in *IEEE Winter Conference on Applications of Computer Vision, WACV*, 2020, pp. 2617–2625.
- [13] C. Gao, G. Cai, X. Jiang, F. Zheng, J. Zhang, Y. Gong, P. Peng, X. Guo, and X. Sun, “Contextual non-local alignment over full-scale representation for text-based person search,” *CoRR*, vol. abs/2101.03036, 2021.
- [14] A. Zhu, Z. Wang, Y. Li, X. Wan, J. Jin, T. Wang, F. Hu, and G. Hua, “DSSL: deep surroundings-person separation learning for text-based person retrieval,” in *The 29th ACM International Conference on Multimedia, MM*, 2021, pp. 209–217.
- [15] Z. Ding, C. Ding, Z. Shao, and D. Tao, “Semantically self-aligned network for text-to-image part-aware person re-identification,” *CoRR*, vol. abs/2107.12666, 2021.
- [16] C. D. Manning, M. Surdeanu, J. Bauer, J. R. Finkel, S. Bethard, and D. McClosky, “The stanford corenlp natural language processing toolkit,” in *The 52nd Annual Meeting of the Association for Computational Linguistics, ACL*, 2014, pp. 55–60.
- [17] S. Li, T. Xiao, H. Li, W. Yang, and X. Wang, “Identity-aware textual-visual matching with latent co-attention,” in *IEEE International Conference on Computer Vision, ICCV*, 2017, pp. 1908–1917.
- [18] D. Chen, H. Li, X. Liu, Y. Shen, J. Shao, Z. Yuan, and X. Wang, “Improving deep visual representation for person re-identification by global and local image-language association,” in *European conference on computer vision, ECCV*, 2018, pp. 56–73.
- [19] K. Niu, Y. Huang, W. Ouyang, and L. Wang, “Improving description-based person re-identification by multi-granularity image-text alignments,” *IEEE Transactions on Image Processing*, vol. 29, pp. 5542–5556, 2020.
- [20] Y. Jing, C. Si, J. Wang, W. Wang, L. Wang, and T. Tan, “Pose-guided multi-granularity attention network for text-based person search,” in *The Thirty-Fourth AAAI Conference on Artificial Intelligence, AAAI*, vol. 34, no. 07, 2020, pp. 11189–11196.
- [21] K. Lee, X. Chen, G. Hua, H. Hu, and X. He, “Stacked cross attention for image-text matching,” in *European Conference on Computer Vision, ECCV*, 2018, pp. 212–228.
- [22] K. Zheng, W. Liu, J. Liu, Z. Zha, and T. Mei, “Hierarchical gumbel attention network for text-based person search,” in *The 28th ACM International Conference on Multimedia, MM*, 2020, pp. 3441–3449.
- [23] Y. Wu, Z. Yan, X. Han, G. Li, C. Zou, and S. Cui, “Lapscore: Language-guided person search via color reasoning,” in *IEEE/CVF International Conference on Computer Vision, ICCV*, 2021, pp. 1624–1633.
- [24] F. Faghri, D. J. Fleet, J. R. Kiros, and S. Fidler, “VSE++: improving visual-semantic embeddings with hard negatives,” in *British Machine Vision Conference, BMVC*, 2018, p. 12.

- [25] C. Liu, Z. Mao, T. Zhang, H. Xie, B. Wang, and Y. Zhang, "Graph structured network for image-text matching," in *IEEE/CVF Conference on Computer Vision and Pattern Recognition, CVPR*, 2020, pp. 10918–10927.
- [26] H. Diao, Y. Zhang, L. Ma, and H. Lu, "Similarity reasoning and filtration for image-text matching," in *The Thirty-Fifth AAAI Conference on Artificial Intelligence, AAAI*, 2021, pp. 1218–1226.
- [27] F. Yang, K. Yan, S. Lu, H. Jia, X. Xie, and W. Gao, "Attention driven person re-identification," *Pattern Recognition*, vol. 86, pp. 143–155, 2019.
- [28] R. Hou, B. Ma, H. Chang, X. Gu, S. Shan, and X. Chen, "Interaction-and-aggregation network for person re-identification," in *IEEE Conference on Computer Vision and Pattern Recognition, CVPR*, 2019, pp. 9317–9326.
- [29] C. Song, Y. Huang, W. Ouyang, and L. Wang, "Mask-guided contrastive attention model for person re-identification," in *IEEE Conference on Computer Vision and Pattern Recognition, CVPR*, 2018, pp. 1179–1188.
- [30] Q. Zhou, B. Zhong, X. Liu, and R. Ji, "Attention-based neural architecture search for person re-identification," *IEEE Transactions on Neural Networks and Learning Systems*, pp. 1–13, 2021.
- [31] X. Qian, Y. Fu, T. Xiang, Y. Jiang, and X. Xue, "Leader-based multi-scale attention deep architecture for person re-identification," *IEEE Transactions on Pattern Analysis and Machine Intelligence*, vol. 42, no. 2, pp. 371–385, 2020.
- [32] K. He, X. Zhang, S. Ren, and J. Sun, "Deep residual learning for image recognition," in *IEEE Conference on Computer Vision and Pattern Recognition, CVPR*, 2016, pp. 770–778.
- [33] J. Deng, W. Dong, R. Socher, L. Li, K. Li, and L. Fei-Fei, "Imagenet: A large-scale hierarchical image database," in *IEEE Computer Society Conference on Computer Vision and Pattern Recognition, CVPR*, 2009, pp. 248–255.
- [34] X. Huang and S. J. Belongie, "Arbitrary style transfer in real-time with adaptive instance normalization," in *IEEE International Conference on Computer Vision, ICCV*, 2017, pp. 1510–1519.
- [35] X. Jin, C. Lan, W. Zeng, Z. Chen, and L. Zhang, "Style normalization and restitution for generalizable person re-identification," in *IEEE/CVF Conference on Computer Vision and Pattern Recognition, CVPR*, 2020, pp. 3140–3149.
- [36] X. Pan, P. Luo, J. Shi, and X. Tang, "Two at once: Enhancing learning and generalization capacities via ibn-net," in *European Conference on Computer Vision, ECCV*, 2018, pp. 484–500.
- [37] J. Hu, L. Shen, and G. Sun, "Squeeze-and-excitation networks," in *IEEE Conference on Computer Vision and Pattern Recognition, CVPR*, 2018, pp. 7132–7141.
- [38] L. Wei, S. Zhang, W. Gao, and Q. Tian, "Person transfer GAN to bridge domain gap for person re-identification," in *IEEE Conference on Computer Vision and Pattern Recognition, CVPR*, 2018, pp. 79–88.
- [39] Y. Wang, C. Bo, D. Wang, S. Wang, Y. Qi, and H. Lu, "Language person search with mutually connected classification loss," in *IEEE International Conference on Acoustics, Speech and Signal Processing, ICASSP*, 2019, pp. 2057–2061.
- [40] J. Liu, Z. Zha, R. Hong, M. Wang, and Y. Zhang, "Deep adversarial graph attention convolution network for text-based person search," in *The 27th ACM International Conference on Multimedia, MM*, 2019, pp. 665–673.
- [41] N. Sarafianos, X. Xu, and I. A. Kakadiaris, "Adversarial representation learning for text-to-image matching," in *IEEE/CVF International Conference on Computer Vision, ICCV*, 2019, pp. 5813–5823.
- [42] K. Niu, Y. Huang, and L. Wang, "Textual dependency embedding for person search by language," in *The 28th ACM International Conference on Multimedia, MM*, 2020, pp. 4032–4040.
- [43] J. Ge, G. Gao, and Z. Liu, "Visual-textual association with hardest and semi-hard negative pairs mining for person search," *CoRR*, vol. abs/1912.03083, 2019.
- [44] T. Chen, C. Xu, and J. Luo, "Improving text-based person search by spatial matching and adaptive threshold," in *IEEE Winter Conference on Applications of Computer Vision, WACV*, 2018, pp. 1879–1887.
- [45] Z. Wang, A. Zhu, Z. Zheng, J. Jin, Z. Xue, and G. Hua, "Img-net: inner-cross-modal attentional multigranular network for description-based person re-identification," *Journal of Electronic Imaging*, vol. 29, no. 4, p. 043028, 2020.
- [46] C. Wang, Z. Luo, Y. Lin, and S. Li, "Text-based person search via multi-granularity embedding learning," in *Proceedings of the Thirtieth International Joint Conference on Artificial Intelligence, IJCAI*, 2021, pp. 1068–1074.
- [47] A. Farooq, M. Awais, J. Kittler, and S. S. Khalid, "Axm-net: Implicit cross-modal feature alignment for person re-identification," in *Thirty-Sixth AAAI Conference on Artificial Intelligence, AAAI*, 2022, pp. 4477–4485.
- [48] S. Woo, J. Park, J. Lee, and I. S. Kweon, "Cbam: Convolutional block attention module," in *European conference on computer vision, ECCV*, 2018, pp. 3–19.
- [49] X. Wang, R. B. Girshick, A. Gupta, and K. He, "Non-local neural networks," in *IEEE Conference on Computer Vision and Pattern Recognition, CVPR*, 2018, pp. 7794–7803.
- [50] R. Arandjelovic, P. Gronat, A. Torii, T. Pajdla, and J. Sivic, "Netvlad: CNN architecture for weakly supervised place recognition," in *IEEE Conference on Computer Vision and Pattern Recognition, CVPR*, 2016, pp. 5297–5307.